FEBS Letters 587 (2013) 1353–1358

journal homepage: www.FEBSLetters.org

Evolutionary conserved motifs constrain the RNA structure organization of picornavirus IRES

Noemí Fernández [1], Lisa Buddrus, David Piñeiro, Encarnación Martínez-Salas *

Centro de Biología Molecular Severo Ochoa, Consejo Superior de Investigaciones Científicas, Universidad Autónoma de Madrid, Cantoblanco, 28049 Madrid, Spain

ARTICLE INFO

Article history:
Received 8 February 2013
Revised 4 March 2013
Accepted 4 March 2013
Available online 15 March 2013

Edited by Michael Ibba

Keywords:
IRES-dependent translation
RNA structure
Conserved motifs
SHAPE reactivity
RNA virus

ABSTRACT

Picornavirus RNAs initiate translation using a 5′ end-independent mechanism based on internal ribosome entry site (IRES) elements. Despite performing similar functions, IRES elements present in genetically distant RNAs differ in primary sequence, RNA secondary structure and trans-acting factors requirement. The lack of conserved features amongst IRESs represents obstacles for the understanding of the internal initiation process. RNA structure is tightly linked to picornavirus IRES activity, consistent with the conservation of RNA motifs. This study extends the functional relevance of evolutionary conserved motifs of foot-and-mouth disease virus (FMDV) IRES. SHAPE structural analysis of mutant IRESs revealed local changes in RNA flexibility indicating the existence of an interactive structure constrained by lateral bulges that maintain the RNA conformation necessary for IRES-mediated translation.

1. Introduction

Translation initiation is a key step in gene expression control. Most eukaryotic mRNAs initiate translation via a 5′-dependent mechanism, which relies on the recognition of the m^{7}GpppN residue (known as cap), located at the 5′ end of cellular mRNAs, by translation initiation factors (eIFs) [1]. In contrast to this manner to initiate protein synthesis, internal ribosome entry site (IRES) elements drive translation initiation using a 5′-independent mechanism in various RNA viruses. Furthermore, a subset of cellular mRNAs also can overcome the inhibition of cap-dependent translation induced by stress conditions (virus infectious, apoptosis, oxidative stress, dysregulated proliferation, amongst others) [2,3]. However, because IRESs differ in nucleotide sequence, RNA secondary structure and trans-acting factors requirement [4–6], deciphering the role of evolutionary conserved motifs is critical to understand internal initiation mechanisms.

Functional and structural analysis of viral IRESs has shown that RNA structure plays a fundamental role for IRES-dependent translation initiation [7–11]. Consistent with this, compensatory substitutions tend to conserve RNA structure during RNA virus evolution [12,13]. Foot-and-mouth disease virus (FMDV) is a member of the *Picornaviridae* family characterized by a high genetic variability all along the genome [14,15], including the IRES region [16]. This feature provides information concerning the tolerance to accept nucleotide substitutions compatible with active RNA [12]. The IRES element of FMDV is located within the long 5′ untranslated region (UTR) (Fig. 1A) upstream of two functional initiator codons [17], both of which are preserved during evolution. The IRES region is organized in structural domains, termed 2 to 5 (or H to L) in 5′ to 3′ direction [18], which are conserved among related viruses [19]. Domains 2, 4, and 5 determine the interaction with eIF4G, eIF4B, eIF3, which are required for initiation of translation in addition to various RNA-binding proteins, also known as IRES-transacting factors (ITAFs) [20–29]. However, the central domain (termed domain 3210 nts in length) has been found to interact with a low number of host factors in comparison to the short domain 5 [30]. This feature is compatible with a large proportion of its bases being hidden within a compact three-dimensional RNA structure. Importantly, the local RNA structure of domain 3 plays a critical role during IRES-dependent translation [7,31]. Moreover, transcripts lacking domain 3 do not promote internal initiation [18]. Despite all these studies, the precise role of domain 3 in IRES-dependent translation is unclear. We have proposed that the basal region of this domain could act as a hub supporting the apical region and keeping it accessible to the ribosomal machinery [12]. In this model, disrupting the RNA structure of the basal and middle region of domain 3 would lead to inactive IRESs.

* Corresponding author. Fax: +34 911964420.
E-mail address: emartinez@cbm.uam.es (E. Martínez-Salas).
[1] Present address: MRC Human Genetics, University of Edinburgh, Crewe Road, Edinburgh EH4 2XU, UK.

0014-5793/$36.00
http://dx.doi.org/10.1016/j.febslet.2013.03.005

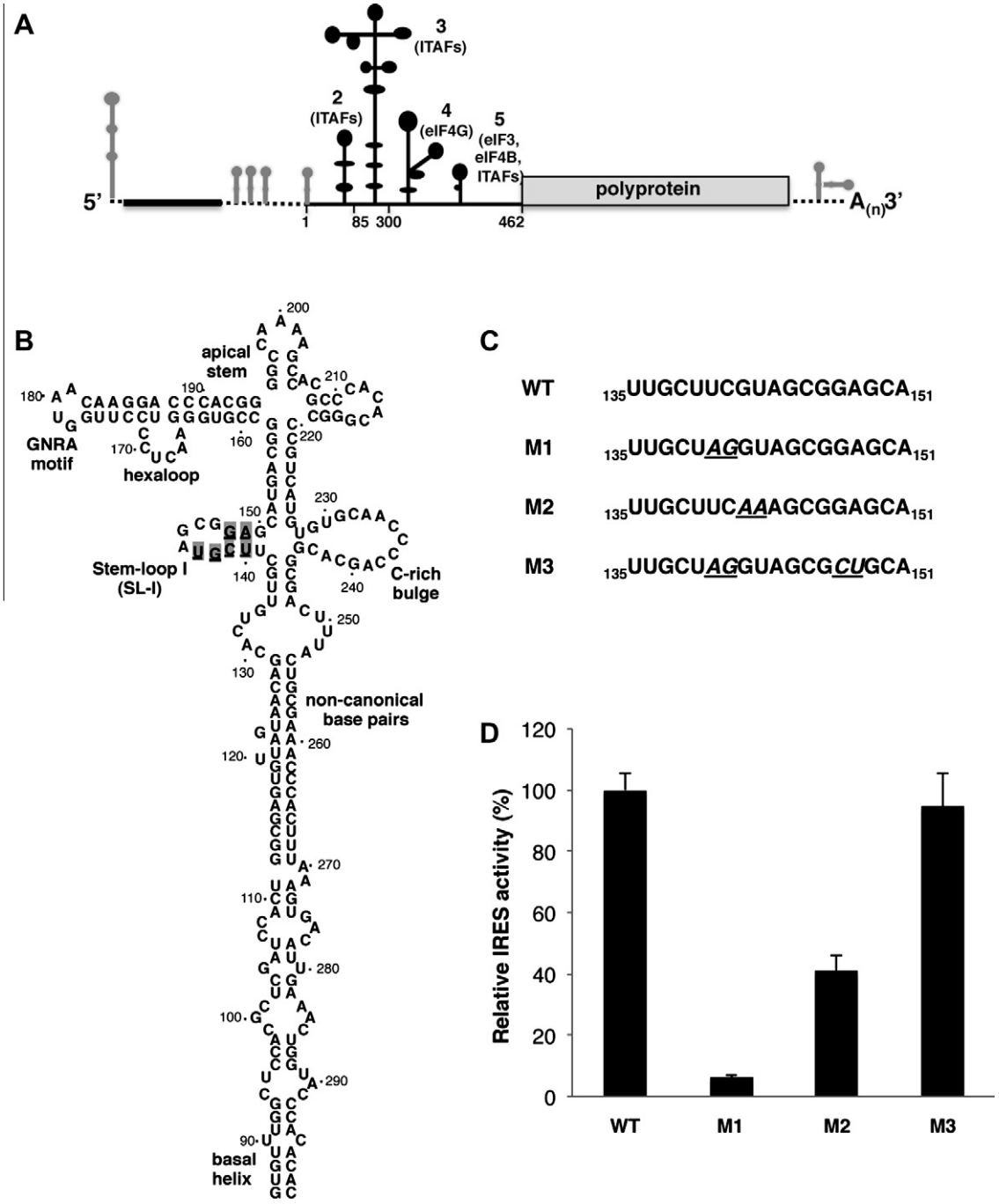

Fig. 1. Mutational analysis of stem-loop I of the IRES element. (A) Schematic representation of the FMDV genome. Grey hairpins depict structural elements located at the 5′ and 3′ ends of the viral RNA. The IRES element and its subdivision in domains are depicted in black; some of the IRES-interacting factors referred to in the text are indicated. For consistency, numbering of the nts conforming the IRES element (1–462) and domain 3 (85–300) are used as in previous works [16]. (B) Secondary structure of domain 3 of the FMDV IRES based on RNA probing data [18]. Nucleotide positions are denoted by dots 10 nt apart. The most relevant motifs referred to in the text are indicated, nucleotides substituted in SL-I are underlined and shaded in grey (C) SL-I nucleotide substitutions (underlined italic letters) present in M1, M2 and M3 mutants are depicted below the corresponding wild type IRES sequence (nt 135–151). (D) Relative IRES activity, determined as the ratio of luciferase to CAT in BHK-21 cells transfected with plasmids of the form CAT-IRES-luciferase made relative to the activity obtained with the wt IRES. Values correspond to the mean of three independent assays. Error bars, S.D.

RNA structure analysis by chemical and enzymatic probing revealed that domain 3 is organized as a cruciform structure [18] including some non-canonical base pairs in the middle region. Earlier studies have shown that conserved motifs in domain 3 play a crucial role in IRES-dependent translation not only in FMDV but also in other type II IRESs found in picornavirus genomes [32–36]. However, while mutations in the conserved GNRA motif or the helical region at the base of domain 3 abrogated IRES activity [32,37], other conserved motifs (such as the C-rich bulge) were tolerant – or not – to nucleotide substitutions depending on the particular substituted nts [31,38]. Thus, the contribution of specific nts to IRES function depends on the structural motif where these nts are located.

Deciphering the structural organization of long IRESs is essential to understanding the mechanism of internal initiation. It is noteworthy that picornavirus IRESs are longer than other viral IRESs [12,39,40]. Their length and flexibility is well suited to structural analysis by selective 2′-hydroxyl acylation analyzed by

primer extension (SHAPE), a technique that has the advantage of allowing the analysis of local RNA flexibility of long RNA molecules [41] shedding light on the RNA organization of the entire regulatory element. SHAPE probing analysis of the FMDV IRES element confirmed its modular organization in structural domains [9]. Furthermore, RNA probing in conjunction with SHAPE reactivity and covariation data [16,18] led us to propose a model of RNA structure for domain 3 that contains internal bulges (Fig. 1B), adopting an RNA structure partially divergent from the one predicted by conventional RNA folding models. To validate the existence of some of these structural elements, we sought to investigate the impact on IRES function of a conserved RNA structural motif encompassing nt 140–150 proposed to fold as an internal bulge held by three base pairs (stem-loop I, SL-I). Mutational analysis was first carried out to investigate the biological relevance of SL-I for IRES activity. Subsequently, SHAPE reactivity analysis revealed the involvement of SL-I in maintaining the local RNA structure of domain 3. The structural changes observed in mutants analyzed in this study supported the existence of an evolutionary conserved RNA structure within domain 3 that performs an essential function during internal initiation.

2. Materials and methods

2.1. Constructs

The construct expressing the IRES RNA was previously described [42]. For consistency, numbering of the nts conforming the IRES element (1–462) and domain 3 (85–300) are used as in previous works [16]. SL-I mutations were generated by overlapping PCR using oligonucleotides NcoIsense (GGCCAATATGGACAACTTC) or pBICsense (CGATGAGTGGCAGGGCGGGGC) for M1 or M2 IRES mutants, respectively, and the antisense primer carrying the mutation (M1 antisense – GCTACCTAGCAACAGTGC; M2 antisense – GCTTTGAAGCAACAGTGC). The resulting products were used in second PCR with pBIC antisense (GGCCTTTCTTTATGTTTTTGGCG), as described [43]. M3 construct was generated by Quick-change method using oligos M3s (GTTGCTAGGTAGCG**CT**GCATGACGGCCGTG) and M3as (CACGGCCGTCATGC**AG**CGCTACCTAGCAAC).

2.2. IRES activity assays

Relative IRES activity was quantified as the expression of luciferase normalized to that of chloramphenicol acetyltransferase (CAT) from bicistronic mRNAs as described [44] in transfected BHK-21 monolayers. Experiments were performed on triplicate wells and each experiment was repeated at least three times.

2.3. RNA synthesis and SHAPE analysis

Plasmids were linearized to generate monocistronic RNAs carrying the full-length IRES using BbuI. Transcription was performed for 1 h at 37 °C using 1000–3000 U of T7 RNA polymerase in the presence of 10–15 μg of linearized DNA template, 40 mM Tris–HCl, 50 mM DTT, 0.5 mM rNTPs, as described [9]. Then, RNA (0.5 pmol) was treated with N-methylisatoic anhydride (NMIA) as described [9]. Equal amounts of NMIA-treated and untreated RNAs (10 μl) were incubated with 0.5 μl of the appropriate antisense 5′ end ^{32}P-labeled primer (5′CTACGAAGCAACAGTG, 5′CCCGGGTGTGGGTACC, 5′GGAATGGGATCCTCGAGCTCAGGGTC, 5′GGCCTTTCTTTATGTTTTTGGCG, or 5′CTACGATCCAACAGTG for M1 RNA). Primer extension was conducted in a final volume of 15 μl containing reverse transcriptase (RT) buffer (50 mM Tris HCl pH 8.3, 3 mM $MgCl_2$, 75 mM KCl, 8 mM DTT), and 1 mM of each dNTP. The mix was heated at 52 °C for 1 min, prior to addition of 100 U of Superscript III RT (Invitrogen) and incubation at 52 °C for 30 min. cDNA products were fractionated in 6% acrylamide, 7 M urea gels, in parallel to a sequence obtained with the same primer.

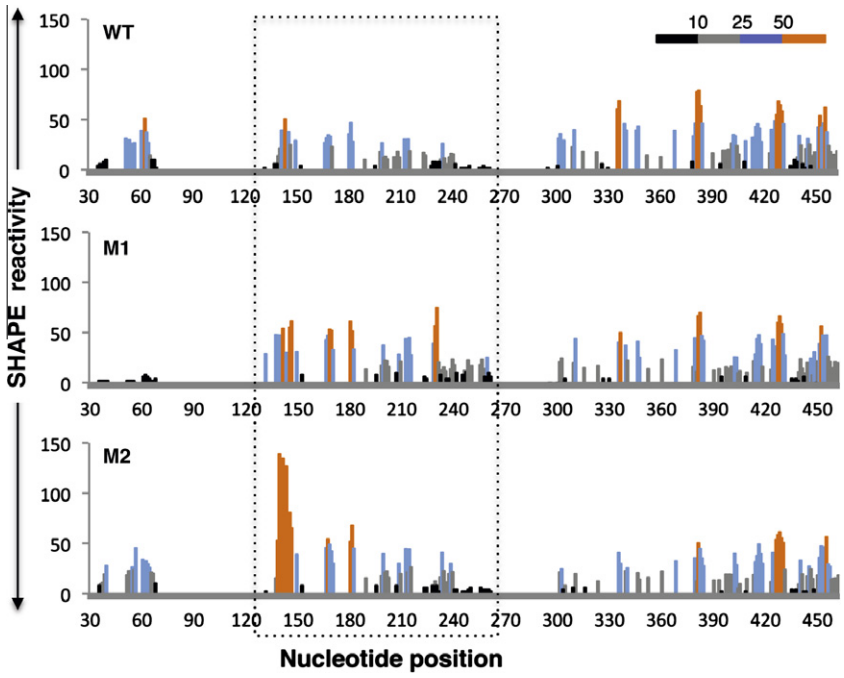

Fig. 2. Impact of sequence composition of SL-I on SHAPE reactivity. SHAPE reactivity of domain 3 IRES mutants. Values of SHAPE reactivity at each individual nucleotide position correspond to the mean reactivity of three independent assays. RNAs, treated with NMIA or untreated, were subjected to primer extension analysis conducted with 5′-end labeled primers. The intensity of each RT-stop band was normalized to the total intensity of the gel lane, made relative to the corresponding full-length product intensity (set to 100%). Then, the background values of the untreated RNA (NMIA−) were subtracted from the respective RT-stop intensity yielded by the treated RNA (NMIA+). Nucleotide positions are indicated on the *x*-axis. The SHAPE reactivity obtained in three independent assays is depicted using color-coded bars.

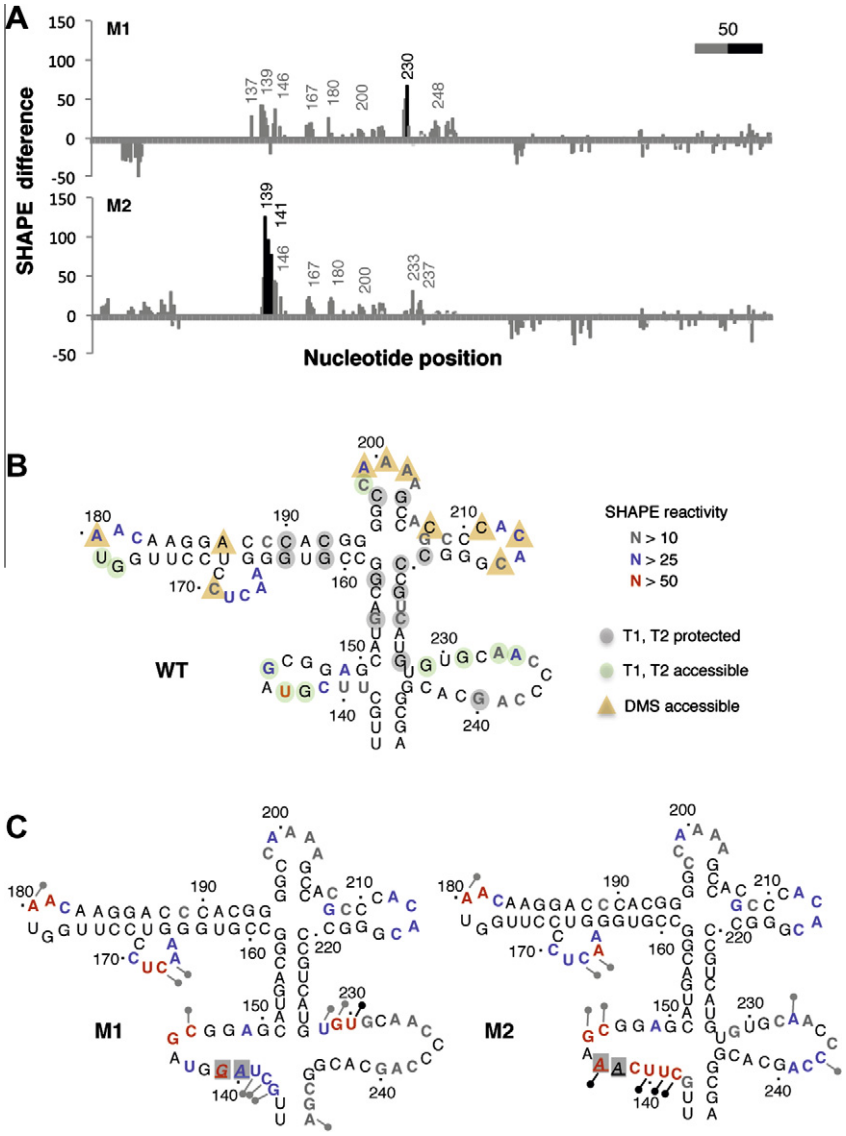

Fig. 3. Modification of the secondary structure of SL-I mutant RNAs. (A) SHAPE difference plots of mutants M1 and M2, relative to the wt RNA. Nucleotides with absolute changes in SHAPE reactivity greater than 50% are depicted in black, while those between 0% and 50% are marked in dark grey. (B) Secondary structure of the apical region of wild type (WT) RNA. Nucleotides are colored as in Fig. 2 to reflect the SHAPE reactivity. For completeness, accessibility or protection to dimethyl sulfate (DMS) and ribonucleases T1 or T2 referred to in the text [31] has been added to the WT RNA. Italic underlined letters depict nucleotide substitutions in M1 and M2 mutants. SHAPE reactivity enhancement or moderate increase is depicted by a black or grey dot-line, respectively. Secondary structure of the apical region of M1 (C) and M2 (D) mutant RNAs deduced from SHAPE reactivity. Symbols are used as in Fig. 3B.

For SHAPE data processing, results from three independent assays were used to calculate the mean SHAPE reactivity. For this analysis, the intensity of each RT-stop band was normalized to the total intensity of the gel lane, made relative to the corresponding full-length product intensity (set to 100%). Then, the background values of the untreated RNA (NMIA−) were subtracted from the respective RT-stop intensity yielded by the treated RNA (NMIA+). To obtain SHAPE differences, the SHAPE reactivity values obtained in the wild type RNA were subtracted from the reactivity values obtained with the mutant RNAs.

3. Results and discussion

Previous analysis of FMDV RNA genetic variability readily indicated an extensive degree of sequence heterogeneity across the IRES element [16]. However, while some regions accumulated a large number of substitutions, others were intolerant to nucleotide changes. We reasoned that the invariant regions could have been subjected to selection pressure to keep their primary sequence due to their involvement in RNA–protein interactions or in maintaining the correct three-dimensional RNA structure. In particular, domain 3 contains three conserved regions encompassing nts 140–150 (the stem-loop I, SL-I), 195–205 (the apical stem-loop), and 229–243 (the C-rich bulge) (Fig. 1B). The latter is a candidate to interact with poly(rC)-binding protein 2 (PCBP2) and ErbB3 binding-protein 1 (Ebp 1, also known as ITAF$_{45}$ and PA2G4) [30,45,46]. Proteins recognizing other regions of this domain have not been identified yet. Notwithstanding, the sequence of these three motifs are conserved in other type II IRESs [46]. These data, aided by the covariation analysis of the FMDV IRES element [16], led us to focus our attention on the conserved SL-I as a candidate region contributing to RNA folding, thus impacting on IRES function.

To determine the biological relevance of SL-I for IRES activity we generated mutants aimed at modifying the sequence of this region

(Fig. 1C). The M1 mutant carrying a double substitution U140C141 to AG, designed to disrupt the canonical U:A, C:G base pairs present in the wild type (WT) IRES, led to a severe loss of IRES activity (5% relative to the wt IRES) (Fig. 1D). In contrast, a double substitution on the bulge, G142U143 to AA (mutant M2) reduced IRES activity to 40%. Interestingly, a compensatory mutation in the stem (mutant M3) led to restoration of IRES activity (94.74%), demonstrating that formation of two consecutive base pairs between U140–C141 and G148–A149 is critical for IRES activity. We conclude that conservation of SL-I is important for IRES activity.

To establish a direct relation between RNA structure and activity of the defective M1 and M2 IRES mutants carrying mutations in SL-I we performed structural analysis by SHAPE that allows the study of long RNA molecules [41]. For this, cDNA products derived from the untreated and NMIA-treated RNAs were resolved in denaturing acrylamide–urea gels in parallel to a sequence ladder obtained with the same primer [9]. In all cases, the mean of three independent assays was used to calculate the values of SHAPE reactivity. The resulting color-coded profiles (Fig. 2) revealed large variations of SHAPE reactivity in domain 3 of M1 and M2 mutants with respect to the wild type (wt) RNA. Specifically, M1 mutant showed enhanced SHAPE reactivity in nts 140–240. Conversely, the enhancement observed in M2 mutant was concentrated in positions 140–150, 170 and 180. SHAPE reactivity observed in domains 2, 4 or 5 was slightly modified, with the exception of nt 60 within domain 2 of M1 mutant, that was protected (Fig. 2). The reasons for this reactivity change remain unknown as no complementarity between these regions of M1 mutant that could explain RNA reorganization was observed. In addition, nts 290–330 were slightly protected in M2 RNA.

To precisely determine the variations in SHAPE reactivity, we plotted the SHAPE differences of the wt RNA with respect to each IRES mutant against the nucleotide position (Fig. 3A). M1 mutant RNA showed an increase in SHAPE reactivity in nts 137–146, as well as nts 228–230 belonging to the C-rich bulge. In addition, moderate SHAPE reactivity enhancements were observed around nts 167 and 180 (the hexaloop and the GNRA motif of domain 3, Fig. 1B), supporting the notion that distant interactions among internal bulges and loops of the apical region constrain the RNA structure of domain 3.

The differences in SHAPE reactivity between M1 and wt RNA led us to suggest interactions between nts located in two lateral bulges (SL-I and C-rich) of domain 3. Specifically, nts 137–146 were more reactive to NMIA (Fig. 3A), indicating that the nts inserted by site directed mutagenesis were unpaired. Besides, nts 228–230 were also more reactive, suggesting a potential interaction between two distant regions of the wt domain 3, which were disrupted in mutant M1. The results derived from SHAPE differences of the M2 RNA pointed to local changes in RNA structure, affecting mainly nts 138–146 (Fig. 3A). Contrary to the increase in SHAPE reactivity of nts belonging to the C-rich bulge observed in M1 RNA, the M2 mutant had similar levels of SHAPE reactivity to the wt RNA with the exception of nt 233 (Fig. 3A). Thus, while disruption of the stem led to a distant effect that reached the adjacent C-rich bulge, changes in the primary sequence of the SL-I loop induced a local RNA reorganization.

Therefore, SL-I plays a crucial role for IRES activity specifically requiring the formation of a stem between U140C141 and G148A149. These results are in agreement with previous chemical and enzymatic accessibility [31] that revealed a lack of attack to these nts while nts 229–234 within the C-rich bulge were accessible to these reagents (Fig. 3B). Interestingly, a feature observed in the IRES mutant M1 studied here is that an increase in reactivity of nts belonging to SL-I was coupled to an enhancement in reactivity around positions 228–233 (Fig. 3C). This result suggests a cross talk between the lateral bulges of domain 3. Although to a lesser extent, this reorganization affected nts located in bulges or loops within the most apical region (Fig. 3D), suggesting that changes in SL-I lead to a loose RNA structure of domain 3.

Our results reinforce the notion that evolutionary conserved motifs have preserved the organization of internal bulges within domain 3 that perform a crucial role in maintaining the correct RNA conformation of the IRES. Mutational analysis revealed that changes in IRES activity were accompanied by a structural reorganization. The results of SHAPE reactivity of wild type and mutant IRES RNAs support a direct effect of nts 140–143 in governing the RNA conformation of the active IRES element. Thus, domain 3 consists of an RNA structure constrained by distant interactions, in which two invariant base pairs within SL-I play a key role in maintaining the correct RNA structure scaffold. It is worth noting that SL-I as well as the adjacent C-rich bulge appears to be conserved during field evolution of the highly variable FMDV genome [16] as well as other type II IRES [46]. Taken together, these results provide further evidence for the crucial role of RNA structure for IRES activity, and reinforce the idea of a distribution of functions between the different IRES structural domains.

Acknowledgments

This work was supported by grant BFU2011-25437 and by an Institutional grant from Fundación Ramón Areces. We are grateful to J. Ramajo for technical assistance. L.B. was an Erasmus student from the University of Surrey (UK).

References

[1] Sonenberg, N. and Hinnebusch, A.G. (2009) Regulation of translation initiation in eukaryotes: mechanisms and biological targets. Cell 136, 731–745.
[2] Spriggs, K.A., Bushell, M. and Willis, A.E. (2010) Translational regulation of gene expression during conditions of cell stress. Mol. Cell 40, 228–237.
[3] Martinez-Salas, E., Pacheco, A., Serrano, P. and Fernandez, N. (2008) New insights into internal ribosome entry site elements relevant for viral gene expression. J. Gen. Virol. 89, 611–626.
[4] Pacheco, A. and Martinez-Salas, E. (2010) Insights into the biology of IRES elements through riboproteomic approaches. J. Biomed. Biotechnol. 2010, 458927.
[5] Belsham, G.J. (2009) Divergent picornavirus IRES elements. Virus Res. 139, 183–192.
[6] Lukavsky, P.J. (2009) Structure and function of HCV IRES domains. Virus Res. 139, 166–171.
[7] Fernandez-Miragall, O. and Martinez-Salas, E. (2003) Structural organization of a viral IRES depends on the integrity of the GNRA motif. RNA 9, 1333–1344.
[8] Costantino, D.A., Pfingsten, J.S., Rambo, R.P. and Kieft, J.S. (2008) TRNA–mRNA mimicry drives translation initiation from a viral IRES. Nat. Struct. Mol. Biol. 15, 57–64.
[9] Fernandez, N., Garcia-Sacristan, A., Ramajo, J., Briones, C. and Martinez-Salas, E. (2011) Structural analysis provides insights into the modular organization of picornavirus IRES. Virology 409, 251–261.
[10] Lukavsky, P.J., Otto, G.A., Lancaster, A.M., Sarnow, P. and Puglisi, J.D. (2000) Structures of two RNA domains essential for hepatitis C virus internal ribosome entry site function. Nat. Struct. Biol. 7, 1105–1110.
[11] Berry, K.E., Waghray, S., Mortimer, S.A., Bai, Y. and Doudna, J.A. (2011) Crystal structure of the HCV IRES central domain reveals strategy for start-codon positioning. Structure 19, 1456–1466.
[12] Martinez-Salas, E. (2008) The impact of RNA structure on picornavirus IRES activity. Trends Microbiol. 16, 230–237.
[13] Nakashima, N. and Uchiumi, T. (2009) Functional analysis of structural motifs in dicistroviruses. Virus Res. 139, 137–147.
[14] Domingo, E., Escarmis, C., Martinez, M.A., Martinez-Salas, E. and Mateu, M.G. (1992) Foot-and-mouth disease virus populations are quasispecies. Curr. Top. Microbiol. Immunol. 176, 33–47.
[15] Carrillo, C., Tulman, E.R., Delhon, G., Lu, Z., Carreno, A., Vagnozzi, A., Kutish, G.F. and Rock, D.L. (2005) Comparative genomics of foot-and-mouth disease virus. J. Virol. 79, 6487–6504.
[16] Fernandez, N., Fernandez-Miragall, O., Ramajo, J., Garcia-Sacristan, A., Bellora, N., Eyras, E., Briones, C. and Martinez-Salas, E. (2011) Structural basis for the biological relevance of the invariant apical stem in IRES-mediated translation. Nucleic Acids Res. 39, 8572–8585.

[17] Lopez de Quinto, S. and Martinez-Salas, E. (1999) Involvement of the aphthovirus RNA region located between the two functional AUGs in start codon selection. Virology 255, 324–336.
[18] Fernandez-Miragall, O., Lopez de Quinto, S. and Martinez-Salas, E. (2009) Relevance of RNA structure for the activity of picornavirus IRES elements. Virus Res. 139, 172–182.
[19] Niepmann, M. (2009) Internal translation initiation of picornaviruses and hepatitis C virus. Biochim. Biophys. Acta 1789, 529–541.
[20] Andreev, D.E., Fernandez-Miragall, O., Ramajo, J., Dmitriev, S.E., Terenin, I.M., Martinez-Salas, E. and Shatsky, I.N. (2007) Differential factor requirement to assemble translation initiation complexes at the alternative start codons of foot-and-mouth disease virus RNA. RNA 13, 1366–1374.
[21] Lopez de Quinto, S., Lafuente, E. and Martinez-Salas, E. (2001) IRES interaction with translation initiation factors: functional characterization of novel RNA contacts with eIF3, eIF4B, and eIF4GII. RNA 7, 1213–1226.
[22] Pacheco, A., Lopez de Quinto, S., Ramajo, J., Fernandez, N. and Martinez-Salas, E. (2009) A novel role for Gemin5 in mRNA translation. Nucleic Acids Res. 37, 582–590.
[23] Luz, N. and Beck, E. (1991) Interaction of a cellular 57-kilodalton protein with the internal translation initiation site of foot-and-mouth disease virus. J. Virol. 65, 6486–6494.
[24] Meyer, K., Petersen, A., Niepmann, M. and Beck, E. (1995) Interaction of eukaryotic initiation factor eIF-4B with a picornavirus internal translation initiation site. J. Virol. 69, 2819–2824.
[25] Stassinopoulos, I.A. and Belsham, G.J. (2001) A novel protein–RNA binding assay: functional interactions of the foot-and-mouth disease virus internal ribosome entry site with cellular proteins. RNA 7, 114–122.
[26] Kolupaeva, V.G., Hellen, C.U. and Shatsky, I.N. (1996) Structural analysis of the interaction of the pyrimidine tract-binding protein with the internal ribosomal entry site of encephalomyocarditis virus and foot-and-mouth disease virus RNAs. RNA 2, 1199–1212.
[27] Kolupaeva, V.G., Pestova, T.V., Hellen, C.U. and Shatsky, I.N. (1998) Translation eukaryotic initiation factor 4G recognizes a specific structural element within the internal ribosome entry site of encephalomyocarditis virus RNA. J. Biol. Chem. 273, 18599–18604.
[28] Clark, A.T., Robertson, M.E., Conn, G.L. and Belsham, G.J. (2003) Conserved nucleotides within the J domain of the encephalomyocarditis virus internal ribosome entry site are required for activity and for interaction with eIF4G. J. Virol. 77, 12441–12449.
[29] Piñeiro, D., Fernandez, N., Ramajo, J. and Martinez-Salas, E. (2013) Gemin5 promotes IRES interaction and translation control through its C-terminal region. Nucleic Acids Res. 41, 1017–1028.
[30] Pacheco, A., Reigadas, S. and Martinez-Salas, E. (2008) Riboproteomic analysis of polypeptides interacting with the internal ribosome-entry site element of foot-and-mouth disease viral RNA. Proteomics 8, 4782–4790.
[31] Fernandez-Miragall, O., Ramos, R., Ramajo, J. and Martinez-Salas, E. (2006) Evidence of reciprocal tertiary interactions between conserved motifs involved in organizing RNA structure essential for internal initiation of translation. RNA 12, 223–234.
[32] Lopez de Quinto, S. and Martinez-Salas, E. (1997) Conserved structural motifs located in distal loops of aphthovirus internal ribosome entry site domain 3 are required for internal initiation of translation. J. Virol. 71, 4171–4175.
[33] Serrano, P., Ramajo, J. and Martinez-Salas, E. (2009) Rescue of internal initiation of translation by RNA complementation provides evidence for a distribution of functions between individual IRES domains. Virology 388, 221–229.
[34] Kuhn, R., Luz, N. and Beck, E. (1990) Functional analysis of the internal translation initiation site of foot-and-mouth disease virus. J. Virol. 64, 4625–4631.
[35] Robertson, M.E., Seamons, R.A. and Belsham, G.J. (1999) A selection system for functional internal ribosome entry site (IRES) elements: analysis of the requirement for a conserved GNRA tetraloop in the encephalomyocarditis virus IRES. RNA 5, 1167–1179.
[36] Witherell, G.W., Schultz-Witherell, C.S. and Wimmer, E. (1995) Cis-acting elements of the encephalomyocarditis virus internal ribosomal entry site. Virology 214, 660–663.
[37] Martinez-Salas, E., Regalado, M.P. and Domingo, E. (1996) Identification of an essential region for internal initiation of translation in the aphthovirus internal ribosome entry site and implications for viral evolution. J. Virol. 70, 992–998.
[38] Martinez-Salas, E., Lopez de Quinto, S., Ramos, R. and Fernandez-Miragall, O. (2002) IRES elements: features of the RNA structure contributing to their activity. Biochimie 84, 755–763.
[39] Filbin, M.E. and Kieft, J.S. (2009) Toward a structural understanding of IRES RNA function. Curr. Opin. Struct. Biol. 19, 267–276.
[40] Lopez-Lastra, M., Ramdohr, P., Letelier, A., Vallejos, M., Vera-Otarola, J. and Valiente-Echeverria, F. (2010) Translation initiation of viral mRNAs. Rev. Med. Virol. 20, 177–195.
[41] Wilkinson, K.A., Gorelick, R.J., Vasa, S.M., Guex, N., Rein, A., Mathews, D.H., Giddings, M.C. and Weeks, K.M. (2008) High-throughput SHAPE analysis reveals structures in HIV-1 genomic RNA strongly conserved across distinct biological states. PLoS Biol. 6, e96.
[42] Ramos, R. and Martinez-Salas, E. (1999) Long-range RNA interactions between structural domains of the aphthovirus internal ribosome entry site (IRES). RNA 5, 1374–1383.
[43] Lopez de Quinto, S. and Martinez-Salas, E. (2000) Interaction of the eIF4G initiation factor with the aphthovirus IRES is essential for internal translation initiation in vivo. RNA 6, 1380–1392.
[44] Lopez de Quinto, S., Saiz, M., de la Morena, D., Sobrino, F. and Martinez-Salas, E. (2002) IRES-driven translation is stimulated separately by the FMDV 3′-NCR and poly(A) sequences. Nucleic Acids Res. 30, 4398–4405.
[45] Walter, B.L., Nguyen, J.H., Ehrenfeld, E. and Semler, B.L. (1999) Differential utilization of poly(rC) binding protein 2 in translation directed by picornavirus IRES elements. RNA 5, 1570–1585.
[46] Yu, Y., Abaeva, I.S., Marintchev, A., Pestova, T.V. and Hellen, C.U. (2011) Common conformational changes induced in type 2 picornavirus IRESs by cognate trans-acting factors. Nucleic Acids Res. 39, 4851–4865.